# Impact of elevated $Ca^{2+}/Mg^{2+}$ concentrations of reverse osmosis membrane desalinated seawater on the stability of water pipe materials

Juan Liang, Anqi Deng, Rongjing Xie, Mylene Gomez, Jiangyong Hu, Jufang Zhang, Choon Nam Ong and Avner Adin

## ABSTRACT

Hardness and alkalinity are known factors influencing the chemical stability of desalinated water. This study was carried out to investigate the effect of $Ca^{2+}$ and $Mg^{2+}$ on corrosion and/or scale formation on the surface of different water distribution pipe materials under tropical conditions. The corrosion rates of ductile iron, cast iron and cement-lined ductile iron coupons were examined in reverse osmosis (RO) membrane desalinated seawater which was remineralised using different concentrations of $Ca^{2+}$ and $Mg^{2+}$. The changes in water characteristics and the coupon corrosion rates were studied before and after the post-treatment. The corrosion mechanisms and corrosion products were examined using scanning electron microscope and X-ray diffraction, respectively. We found that the combination of $Ca^{2+}$ and $Mg^{2+}$ (60/40 mg/L as $CaCO_3$) resulted in lower corrosion rates than all other treatments for the three types of pipe materials, suggesting that $Ca^{2+}/Mg^{2+}$ combination improves the chemical stability of desalinated seawater rather than $Ca^{2+}$ only.

**Key words** | $Ca^{2+}/Mg^{2+}$, corrosion, desalinated water, post-treatment, remineralisation, water distribution pipeline

**Juan Liang**
**Anqi Deng**
**Jiangyong Hu**
**Jufang Zhang**
**Choon Nam Ong**
National University of Singapore,
NUS Environment Research Institute,
5A Engineering Drive 1, T-Lab Building #02-01,
Singapore 117411,
Singapore

**Rongjing Xie** (corresponding author)
**Mylene Gomez**
Technology Department, the Public Utilities Board,
80/82 Toh Guan Road East, #C4-03,
Singapore 60857,
Singapore
E-mail: *xie_rongjing@pub.gov.sg*

**Avner Adin**
Department of Soil and Water Sciences,
Faculty of Agriculture, Food and Environment,
The Hebrew University of Jerusalem,
Rehovot 76100,
Israel

## INTRODUCTION

Pipeline corrosion in drinking water distribution systems is of special concern because of various related problems (Lee & Schwab 2005). First, pipe mass is lost through leaching or oxidisation to soluble species or insoluble scales, which shortens pipe lifetime and increases the maintenance costs. Second, the scale can accumulate as large tubercles that increase head loss, decrease water capacity, and thus increase pumping costs. Finally, while having health impacts on consumers, the release of soluble or particulate corrosion by-products to the water decreases its aesthetic quality and often leads to consumer complaints of 'red water' at the tap. Iron pipe corrosion usually results in water quality with a red, brown or yellow colour, or a dirty appearance. Corrosion products also provide habitats for microbial growth and react with disinfectant residuals, preventing the disinfectant from penetration of biofilm.

In recent years, seawater desalination has become one of the most important water resources, especially in coastal regions with insufficient fresh water supply. However, the soft product water is chemically unstable and the corrosiveness of the desalinated water threatens the service life of the water distribution pipelines. To prevent corrosion from happening and to control the water quality for drinking and other purposes, post-treatment of desalinated water is required (Hasson & Bendrihem 2006; Lahav & Birnhack 2008; Birnhack *et al.* 2011). Various post-treatment methods include direct chemical dosage, blending with other water, calcite/dolomite dissolution to increase pH, alkalinity and buffering capacity. Most of them can provide calcium iron but few methods offer magnesium mineral.

Traditionally, the chemical stability of drinking water is a function of the value of three factors: (1) the

doi: 10.2166/wh.2013.060

buffering capacity or alkalinity of the water, i.e., the ability of the water to withstand substantial changes in pH when a base or an acid is added to it; (2) the propensity of the water to precipitate $CaCO_3$, which can be described by a variety of qualitative (e.g., the Langelier) and/or quantitative (e.g., the calcium carbonate precipitation potential, CCPP) indices; and (3) the concentration of soluble $Ca^{2+}$ or other ions of multivalences in the water.

On the other hand, calcium is an element that is vital for human growth and health (Chiu *et al.* 2011). A minimal $Ca^{2+}$ concentration value is required for health reasons and has been typically set at 50 to 60 mg/L as $CaCO_3$. The maximum value is due to economic reasons attributed to the need to supply water that is not excessively hard. The range for $Ca^{2+}$ values thus lies roughly between 50 and 120 mg/L as $CaCO_3$ (Anthony 2005). Magnesium is also an element which is vital to health because, as research has shown, it maintains the heartbeat and thus prevents heart attacks. It is estimated that each year several hundred lives would be saved by regular consumption of magnesium in desalinated water, regular rainwater or bottled mineral water. In 2009 the Israeli Ministry of Health decided to add a minimum requirement of 10 mg $Mg^{2+}$/L to the criteria due to the acknowledged importance that $Mg^{2+}$ ions have on both crop quality and public health (Catling *et al.* 2008). The World Health Organization (WHO) has recently recommended a minimum concentration of 10 mg $Mg^{2+}$/L in all drinking waters, with special emphasis on desalinated water (WHO 2009). This recommendation is based on recent publications which stress the role of $Mg^{2+}$ in drinking water on the human body and the possible implications of $Mg^{2+}$ deficiency on public health (Kozisek 2003; Cotruvo 2006).

Seawater reverse osmosis (SWRO) products remineralised by $Ca^{2+}$ have been proven to be capable of reducing iron corrosion (Liang *et al.* 2013). However, little information is available in the literature on the combined effect of $Ca^{2+}/Mg^{2+}$ on the corrosion and scale formation of desalinated water on the surface of water pipes, especially Singapore tropical underground water distribution pipelines (28–29 °C). Specific attention was paid to the effect of $Mg^{2+}$ as this cation has rarely been investigated in drinking water distribution pipelines.

## METHODOLOGY

In this study, three types of pipeline materials (ductile iron, cast iron and cement-lined ductile iron) were explored to investigate the effect of $Ca^{2+}/Mg^{2+}$ remineralised reverse osmosis (RO) membrane desalinated seawater on the stability of the pipe materials. Traditionally, cast iron was a widely existing pipe material for water and wastewater transport. Ductile iron is one of the most commonly used pipe materials in modern infrastructure for water distribution, while cement-lined ductile iron pipe has excellent anti-corrosion properties because cement lining provides a barrier between the water and the iron pipe, reducing the pipe's susceptibility to corrosion (Bonds 2005).

Ductile iron, cast iron and cement-lined ductile iron were selected as representative pipe materials. Rectangular metal coupons with the dimensions of 40 mm × 13 mm × 2 mm and with a 5 mm diameter hole at one end were prepared following the standard method (ASTM G1-90 1999). As shown in Table 1, chemical compositions of ductile iron and cast iron are similar. Both were made of Fe >92% and C 3.7%. For the cement-lined ductile iron coupons, the coupons were coated with 0.5 mm cement, of which the elemental compositions are CaO (52.7%), $SiO_2$ (24%), $Al_2O_3$ (8.9%), $Fe_2O_3$ (3.5%), MgO (2.5%) and others.

Triplicate coupons of either ductile iron, cast iron or cement-lined ductile iron were immersed in 1-L glass reactors with 800 mL desalinated water in temperature-controlled incubators. The temperature was kept at 28–29 °C, similar to that of water in Singapore underground water distribution pipelines. Fifteen reactors were filled with remineralised RO membrane desalinated seawater. SWRO product was taken

**Table 1** | Coupon composition of ductile iron, cast iron and cement liner

| Element, Wt % | Ductile iron | Cast iron | Composition, Wt % | Cement liner |
|---|---|---|---|---|
| Fe | 96.84 | 92.36 | S | 2.2 |
| Si | 0.98 | 2.13 | $SiO_2$ | 24 |
| Mn | 0.27 | 0.23 | CaO | 52.7 |
| P | 0.18 | 0.24 | $Al_2O_3$ | 8.9 |
| Mg | NA | NA | $Fe_2O_3$ | 3.5 |
| C | 3.70 | 3.63 | MgO | 2.5 |
| S | <0.50 | <0.50 | $K_2O$ | 1 |

NA: not available.

from the Singapore variable salinity plant, Tampines. As shown in Table 2, SWRO product was remineralised with various chemicals to a concentration level slightly above the minimum standard based on economic concern. The experiments were carried out following the standard procedures of laboratory immersion corrosion tests (ASTM G1-90 1999; ASTM G31-72 1999). The corrosion phenomenon was monitored during the whole process. After 497 hours' immersion, all coupons were taken out of the reactors, dried, cleaned and weighed for corrosion rate calculation. According to the ASTM standard, each coupon was rinsed with a forceful stream of cold tap water to remove residual test solution and loose corrosion products. Subsequently, the coupons were immersed in a chemical cleaning solution (500 mL HCl + 3.5 g $(CH_2)_6N_4$) for 10 min to remove attached corroded oxide film, and then water rinsed and oven dried. Finally, the coupons were mechanically cleaned by grit paper if persistent residues remained and then weighed after rinsing with water.

Water was filtered using 0.8 μm filter paper to remove particulates. Water characteristics, such as pH, total alkalinity, total hardness and total dissolved solids (TDS), were measured before and after the treatment. Concentrations of $Ca^{2+}$ and $Mg^{2+}$ were analysed using inductively coupled plasma optical emission spectrometer (ICP-OES, Optima 7000 DV, Perkin Elmer). Coupon surface was observed using scanning electron microscope (SEM, Stereoscan 420, Leica, Cambridge Instruments).

Compositions of the powder samples from the corrosion layer and bottom of the reactors were analysed using the D5005 Bruker powder X-Ray diffractometer. Full X-ray diffraction patterns were recorded for the scan angles (2θ) from 10° to 80° with step size 0.02° to identify iron oxides.

## RESULTS AND DISCUSSION

### Corrosion phenomena

As shown in Figure 1, after being immersed in the SWRO membrane product water, the iron coupons were subjected

**Table 2** | Character of tested water qualities

| Tested water | Post-treatment | pH adjustment | Alkalinity addition (mg/L as $CaCO_3$) | $Ca^{2+}$ addition | $Mg^{2+}$ addition |
|---|---|---|---|---|---|
| SWRO | None | 7.25 | 0 | 0 | 0 |
| SWRO with pH adjustment | NaOH | 8 | 0 | 0 | 0 |
| Remineralised SWRO | $NaHCO_3 + CO_2$ | 8 | 100 | 0 | 0 |
| | $Ca(OH)_2 + CO_2$ | 8 | 100 | 100 | 0 |
| | $Ca(OH)_2 + MgCO_3 + CO_2 + NaHCO_3$ | 8 | 100 | 60 | 40 |

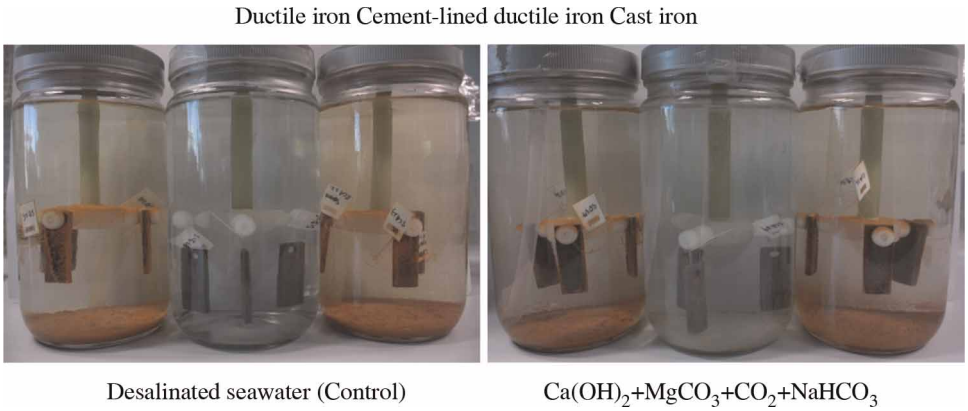


**Figure 1** | Corrosion phenomena of different iron coupons for control and remineralised water after 497 hours of immersion tests.

to corrosion and a layer of red substances started forming on the surfaces of the coupons and some crust gradually settled at the bottoms of the reactors. Water colour in all reactors with iron coupons became greenish on the second day and orange from the third day onwards (photographs not shown). No red precipitate was observed in the reactors with cement-lined coupons while white precipitate was found in treatments with $Ca^{2+}/Mg^{2+}$ or $CO_3^{2-}$ additions. The white precipitate was dissolved by HCl solution (4 mL 10% HCl + 300 mL ultra pure water) and analysed by ICP-OES. $CaCO_3$ appeared and attributed to high $Ca^{2+}$ concentration. The white precipitate $CaCO_3$ was not found in the reactors for the controls (i.e., SWRO permeate only) and for the SWRO membrane permeate for which only pH was adjusted.

## Corrosion rate comparison

The simplest and longest established method of estimating corrosion losses in plant and equipment is weight loss analysis. A weighed sample (coupon) of the metal or alloy under consideration is introduced into the process, and later removed after a reasonable time interval. The coupon is then cleaned of all corrosion products and is reweighed. The weight loss is converted to a corrosion rate (CR) as follows (ASTM G31-72 1999):

$$\text{Corrosion rate} = (K \times W)/(A \times T \times D)$$

where: $K$ = a constant, $T$ = time of exposure in hours, $A$ = area in $cm^2$, $W$ = mass loss in grams, and $D$ = density in $g/cm^3$.

Many different units are used to express corrosion rates. Using the above units for $T$, $A$, $W$ and $D$, the corrosion rate can be calculated in a variety of units with the corresponding appropriate value of $K$. In this study, mils per year (mpy; 1 mils = 1/1,000 inch = 0.0254 mm) is used as the unit of corrosion rate and the constant $K$ is $3.45 \times 10^6$. Corrosion rate was calculated for each water sample tested and presented in Figure 2.

Comparison of the corrosion rates of different pipeline materials showed that cement-lined ductile iron had the lowest while cast iron had the highest corrosion rate regardless of how the desalinated seawater was post-treated. As for the post-treatment methods, remineralisation of the water using $Ca^{2+}/Mg^{2+}$ produced the lowest corrosion rate compared with all the other treatments for ductile iron, cast iron and cement-lined ductile iron materials. The combined $Ca^{2+}/Mg^{2+}$ appeared to have effectively reduced the corrosion (Figure 2). However, the reduction of corrosion by addition $Ca^{2+}/Mg^{2+}$ was significant to cast iron, less significant to ductile iron and slightly significant to cement-lined iron coupons.

Other researchers also reported similar results but without $Mg^{2+}$ addition (Chang 2004; Hasson & Bendrihem 2006; Douglas 2007; Birnhack *et al.* 2011). Chang (2004) studied three post-treatment processes, namely lime and carbon dioxide, sodium bicarbonate or carbonate and alkaline media filter, to reduce the corrosiveness of the product from the desalination plant using ductile iron coupons.

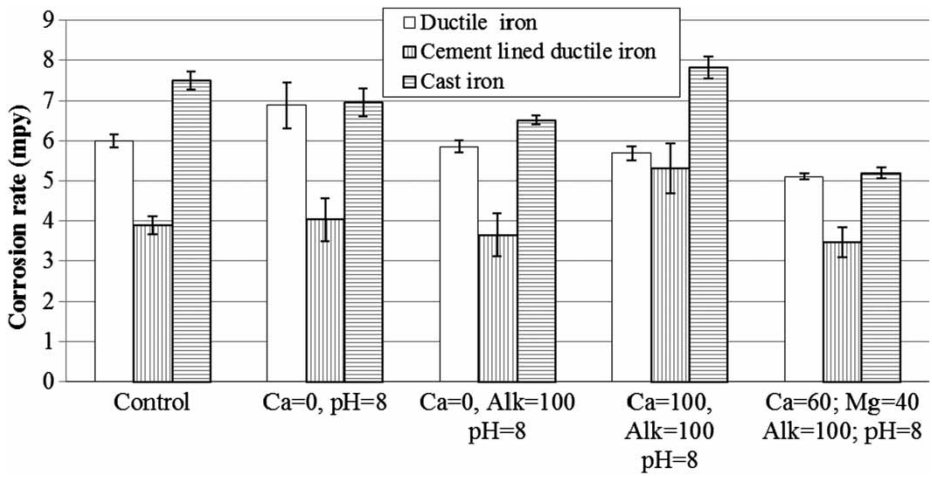


**Figure 2** | Corrosion rate of different coupons as related to various post-treatments of corrosive SWRO permeate.

The results showed that lime and carbon dioxide were very efficient to chemically stabilise the corrosive water.

$Mg^{2+}$ is a recent public health concern (WHO 2009) and so far most of the corrosion studies have been focused on the effect of $Ca^{2+}$. Based on our knowledge, no studies have been conducted on the effect of $Mg^{2+}$ on pipeline material corrosion. Our results revealed that the combination of $Ca^{2+}$ and $Mg^{2+}$ significantly reduced the coupon corrosion rate. Therefore, post-treatment combining $Ca^{2+}/Mg^{2+}$ can be a preferred option instead of calcium alone. However, in the engineered post-treatment methods, only dolomite dissolution can provide small amounts of $Mg^{2+}$ (Birnhack *et al.* 2011). Several problems are encountered when attempting to dissolve dolomite rocks ($MgCa(CO_3)_2$) for this purpose. The most noticeable drawback is the dissolution kinetics of dolomite, which is much slower than that of calcite (Liu *et al.* 2005). As a result, either a much larger reactor volume, longer hydraulic retention times or lower pH is required to dissolve an adequate amount of $Mg^{2+}$ ions. If the initial pH is low, NaOH would be required to elevate the alkalinity and CCPP values, and often the limit for pH (i.e., pH 8.5) would be exceeded. Another problem associated with dolomite is that the $Ca^{2+}$ to $Mg^{2+}$ ratio released during its dissolution tends not to be constant with time because excavated dolomite minerals are rarely pure, and the $CaCO_3$ component within the dolomite structure tends to dissolve more rapidly than the $MgCO_3$ component (Liu *et al.* 2005).

A novel post-treatment approach for desalinated water, aimed at supplying a balanced concentration of alkalinity, $Ca^{2+}$, $Mg^{2+}$ and $SO_4^{2-}$, has been developed (Birnhack & Lahav 2007; Penn *et al.* 2009; Birnhack *et al.* 2010). The process is based on replacing excess $Ca^{2+}$ ions generated in the common $H_2SO_4$-based calcite dissolution post-treatment process with $Mg^{2+}$ ions originating from seawater. The exchange is complemented using a specific ion exchange resin that has high affinity toward divalent cations to meet a predetermined $Ca^{2+}$ to $Mg^{2+}$ ratio. The proposed process allows for the supply of cheap $Mg^{2+}$ ions, thus resulting in higher quality water at a cost-effective price.

## SEM microstructure

The microstructure of coupons before and after the treatments was observed using SEM (Figure 3). Before the treatment, the surfaces of ductile iron and cast iron coupons were even with some small cavities. After the treatments, the coupon surfaces became rough with pits. The corrosion mechanisms that were predominant for ductile iron and cast iron appeared to be uniform and identified as pitting corrosion (Reynaud 2010).

Cement-mortar lining provided a barrier between the water and the pipe material reducing its susceptibility to corrosion conditions. Two main mechanisms could influence the degradation kinetics of cement lining: (1) ion transfers between the bulk water and the pore water; and (2) chemical reaction between the water and components of the cement (Adenot & Buil 1992).

Figures 4 and 5 show the comparisons of cement-lined ductile iron coupons before and after corrosion tests. The surface looked smoother after testing compared against the rough surface before test (Figure 4), probably due to cement dissolution when the coupon was submersed in water. However, when the cement liner was removed, pitting corrosion was evident owing to the presence of numerous rusty dots on the iron surface (Figure 5). Desalinated seawater permeated the pores of the liner causing the pitting corrosion phenomenon observed on the iron surface. Desalinated water permeated into the liner perhaps because the cement liner that was used was very thin (0.5 mm) and thickness not being unique. In practical applications, cement lining in actual pipes is packed more densely and thicker than what was used in this project.

Figure 6 shows the SEM images of corroded ductile iron before chemical and physical cleaning in water treated with $Ca^{2+}$ only. For the surface covered by orange corrosion substances, some composites colonised together cloudily. Some crystals shaped in fibre or blocks were found on the surface without orange iron corroded products. The crystal precipitate was calcite or aragonite components. They might have formed a layer blocking further corrosion on this portion.

## Scales

The corrosion products formed on the iron surface have a complex morphology. The exact composition and structure of iron corrosion scales, however, varies significantly with water qualities, flow properties as well as other environmental parameters. Typical iron corrosion products

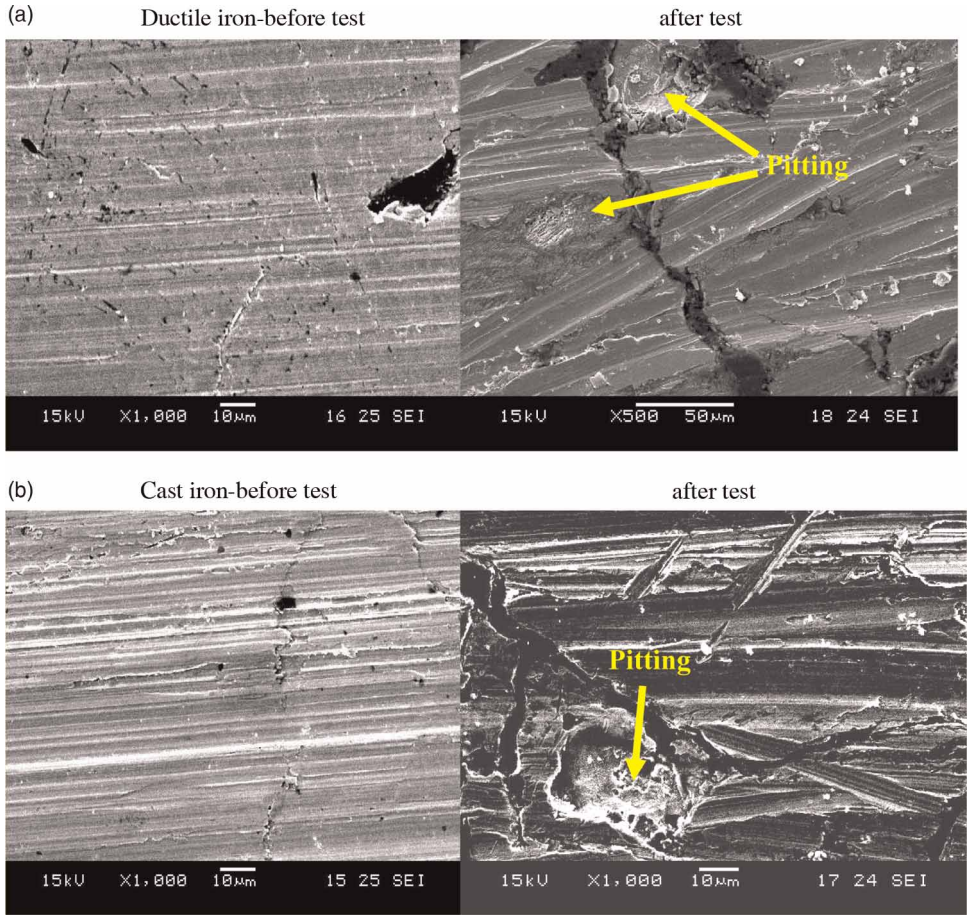


**Figure 3** | SEM images showing comparison of ductile and cast iron before and after the corrosion test.

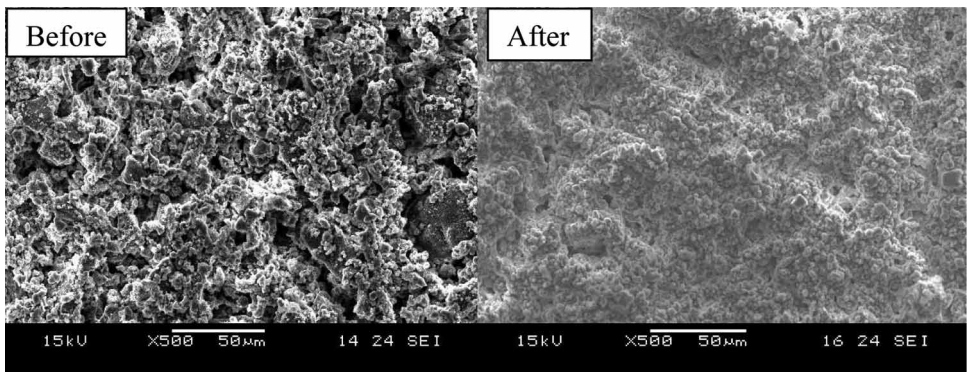


**Figure 4** | SEM images of cement lining before and after corrosion treatment.

formed on aged pipe surfaces can be described using three different layers: (a) a macroporous layer of black rust (magnetite, $Fe_3O_4$) in contact with the metal; (b) a microporous film of a mixture of $Fe^{2+}$ and $Fe^{3+}$ species that covers the macro-layer; and (c) a top layer of red rust (mainly goethite, a-FeOOH and hematite, a-$Fe_2O_3$), which is generally porous with poor adherence (Sarin *et al.* 2004; Tang *et al.* 2006; Gerke *et al.* 2008).


**Figure 5** | Comparison of the ductile iron coupons with and without corrosion after testing and the removal of cement lining.

In our study, the corrosion products were found to be similar in composition to that of the outer surface layer previously described (Table 3). There were no obvious differences of the corrosion products between ductile iron and cast iron. Rust crusts found on the coupon surfaces were composed of FeO(OH) [lepidocrocite], $Fe(OH)_3$ and other iron components. In $Ca(OH)_2$ or $MgCO_3$ treated water, calcium compounds (CaO, $CaO_2$, $CaCO_3$) and $MgO_2$ were detected in the corroded scales. A few tiny white granules, which were believed to be calcium deposits, were also found on some iron coupon surfaces.

## Water quality

Various water quality parameters before and after remineralisation are presented in Figure 7. Total alkalinity, total hardness, pH, TDS, redox potential, conductivity and $Ca^{2+}$ increased considerably with cement-lined ductile iron due to cement dissolution. In a study by Bonds (2005), extended contact under high-flow conditions initially accelerated leaching of cement-mortar lining but the changes in water quality were not noticeable due to the constant water dilution. In our study, however, extended contact between the water and the lining material significantly changed the water quality inside the reactor, including pH (not shown), alkalinity and calcium concentration, because the water in the reactor was not replaced during the experiment.

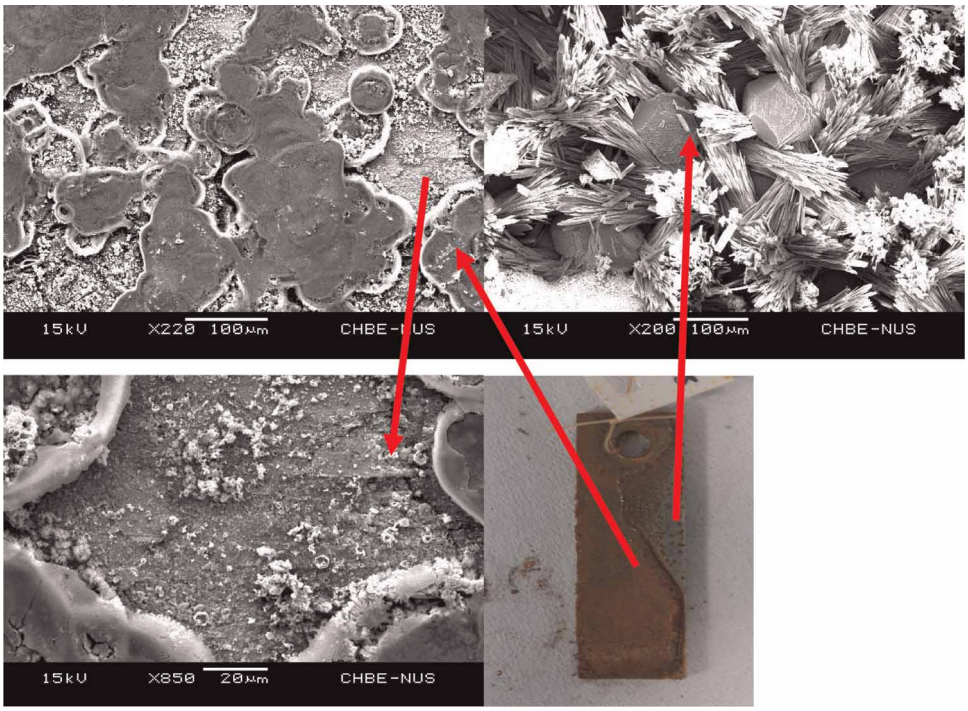


**Figure 6** | SEM images of dust and precipitation on ductile iron coupon surface.

**Table 3** | Corrosion products of ductile iron and cast iron identified using X-ray diffraction

| Tested water | Ductile iron | Cast iron |
|---|---|---|
| SWRO permeate (Control) | $FeO(OH)$, $Fe(OH)_3$ | $FeO(OH)$, $Fe(OH)_3$ |
| | Fe0.98O, FeO | FeOOH, Fe0.98O |
| $Ca = 0$, $pH = 8$; (NaOH) | $FeO(OH)$, $Fe(OH)_3$ | $FeO(OH)$, $Fe(OH)_3$ |
| | Fe0.98O,FeO, $Fe_2O_3$ | Fe0.98O, $Fe_2O_3$ , FeO |
| | $FeFe_2O_4$ | |
| $Ca = 100$, $Alk = 100$, $pH = 8$; $Ca(OH)_2 + CO_2 + NaHCO_3$ | $FeO(OH)$, $Fe(OH)_3$ | $FeO(OH)$, $Fe(OH)_3$ |
| | FeOOH, $Fe_2O_3$, $Fe_2O_3$ | FeOOH, $Fe_2O_3$ |
| | CaO,$CaO_2$,$CaCO_3$ | CaO, $CaCO_3$ |
| $Ca = 60$, $Mg = 40$, $Alk = 100$, $pH = 8$; $Ca(OH)_2 + MgCO_3 + CO_2$ | $FeO(OH)$, $Fe(OH)_3$ | $FeO(OH)$, $Fe(OH)_3$ |
| | FeOOH, Fe0.98O, $Fe_2O_3$, | FeOOH, $Fe_2O_3$, |
| | CaO, $CaCO_3$, $MgO_2$ | CaO, $CaCO_3$, $MgO_2$ |

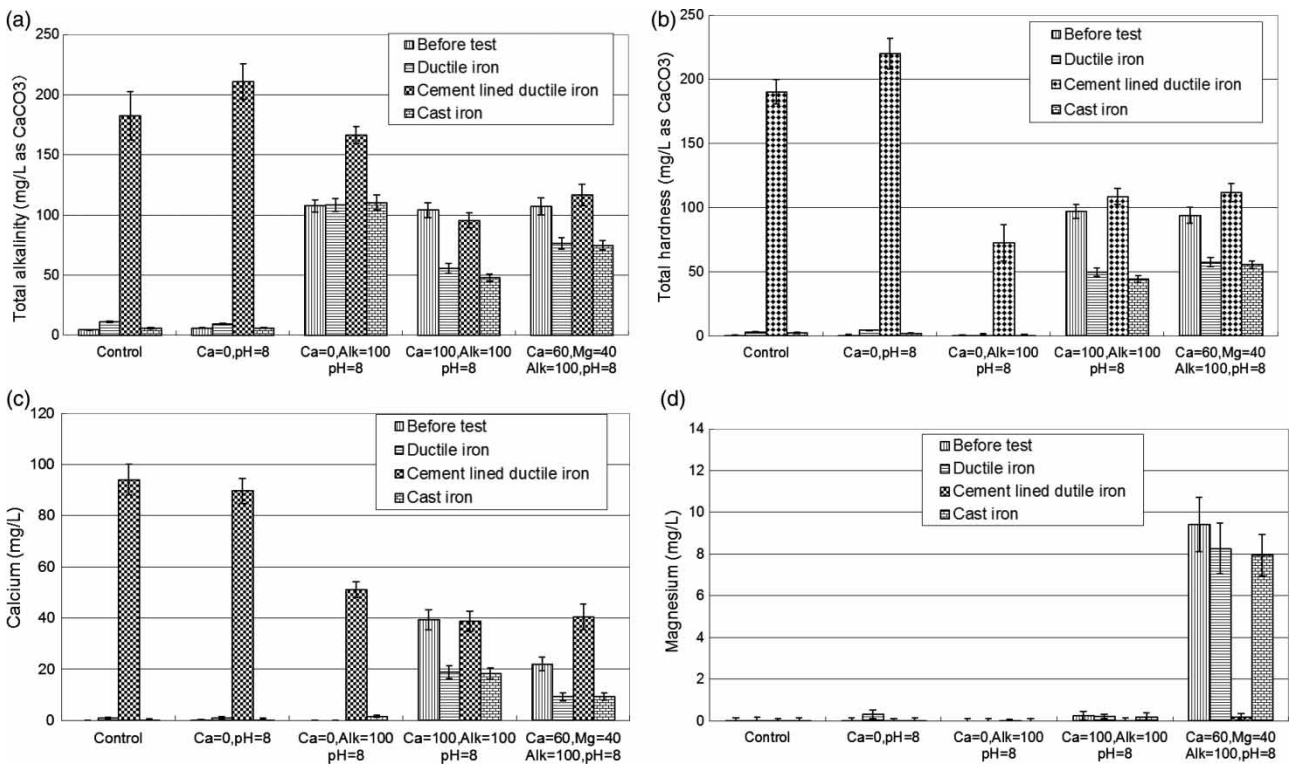


**Figure 7** | Changes in water quality before and after the post-treatments. (a) Total alkalinity, (b) total hardness, (c) calcium concentration, (d) magnesium concentration.

It was noted that the $Mg^{2+}$ concentrations, however, decreased from 9.42 to 0.20 mg/L. To verify these changes on ion concentrations before and after the test, $Ca^{2+}/Mg^{2+}$ balance was calculated for remineralised water with cement-lined coupons and the results are shown in Table 4. The collected $Ca^{2+}$ is much higher than the original amount, which means cement dissolution releasing $Ca^{2+}$ to the water. For treatment with $MgCO_3$, some substances

**Table 4** | $Ca^{2+}$ and $Mg^{2+}$ mass balance for selected post-treatments

| | $Ca^{2+}$ (mg) | | $Mg^{2+}$ (mg) | |
|---|---|---|---|---|
| **Water quality** | **Original** | **Recovered** | **Original** | **Recovered** |
| Ca = 100, pH = 8 | 28.74 | 151.94 | 0.20 | 0.47 |
| Ca = 60, Mg = 40, pH = 8 | 18.56 | 102.73 | 8.27 | 5.53 |

Recovered: left on the filter paper + deposit at bottle bottom + in water.

containing $Mg^{2+}$ (5.53 mg) were deposited at the reactor bottom and on the filter paper even though $Mg^{2+}$ concentration was close to zero in the water. The water in the reactor was filtered through 0.8 μm membrane paper, and some white suspended solids from the water remained on the filter paper surface which proved to be $Mg^{2+}$ compounds by ICP-OES. At the same time, some $Ca^{2+}/Mg^{2+}$ deposits could be washed away during the washing stage after the coupons were taken out of the reactors. Therefore, the quantity of recovered $Mg^{2+}$ (5.53 mg) was lower than the added amount (8.27 mg).

For iron coupons in the water treated with $Ca(OH)_2 + CO_2$ or $Ca(OH)_2 + MgCO_3 + CO_2 + NaHCO_3$, the water characteristics were similar before and after the remineralisation process except for hardness, alkalinity, $Ca^{2+}$ and $Mg^{2+}$ concentrations. Total alkalinity, total hardness, $Ca^{2+}$ and $Mg^{2+}$ concentrations decreased after 497-hour corrosion tests probably as a result of $CaCO_3/MgCO_3$ precipitation. Concentration of $Mg^{2+}$ marginally decreased from 9.42 mg/L to ~8 mg/L in water without cement-lined coupons (Figure 7(d)), while the difference was 9.22 (9.42 – 0.20) mg/L in the water with cement-lined coupons. It indicates much more $Mg^{2+}$ precipitation in water with cement-lined coupons due to cement dissolution. According to Figure 7(d) and Table 4, the $Mg^{2+}$ ions were precipitated as a result of reaction with the cement lining, which probably explains why their effect is slightly significant to cement-lined iron coupons which were shown in Figure 2 earlier.

## CONCLUSIONS

This study led to several observations with elevated $Ca^{2+}/Mg^{2+}$ concentration in remineralised SWRO membrane product water in comparison with the control for ductile iron, cast iron and cement-lined ductile iron pipe materials. Of the corrosion rates for different post-treatments, desalinated water treated with $Ca^{2+}/Mg^{2+}$ led to the lowest corrosion rate for all three pipe materials. The combination of $Ca^{2+}$ and $Mg^{2+}$ further reduced pipe corrosion in comparison with $Ca^{2+}$ alone. Therefore, addition of both $Ca^{2+}$ and $Mg^{2+}$ is recommended for the post-treatment because of the benefits both to human health and in mitigating pipeline corrosion.

## ACKNOWLEDGEMENTS

This research was financially supported by Environment and Water Industry (EWI), Public Utilities Board (PUB) and National University of Singapore (NUS). The authors would also like to acknowledge the water supply from PUB's variable salinity plant and NUS Environment Research Institute (NERI)/NUS staff for providing technical support to this project.

## REFERENCES

Adenot, F. & Buil, M. 1992 Modelling of the corrosion of the cement paste by deionized water. *Cement Concrete Res.* **22** (2–3), 489–496.

Anthony, W. 2005 Options for recarbonation, remineralisation and disinfection for desalination plants. *Desalination* **179** (1), 11–24.

ASTM G1–90 1999 Standard practice for preparing, cleaning, and evaluating corrosion test specimens. *Annual Book of ASTM Standards*, Vol 03.02.

ASTM G31–72 1999 Standard practice for laboratory immersion corrosion testing of metals. *Annual Book of ASTM Standards*, Vol 03.02.

Birnhack, L. & Lahav, O. 2007 A new post treatment process for attaining $Ca^{2+}$, $Mg^{2+}$, $SO_4^{2-}$ and alkalinity criteria in desalinated water. *Water Res.* **41** (17), 3989–3997.

Birnhack, L., Penn, R., Oren, S., Lehmann, O. & Lahav, O. 2010 Pilot scale evaluation of a novel post-treatment process for desalinated water. *Desalination Water Treat.* **13**, 120–127.

Birnhack, L., Voutchkov, N. & Lahav, O. 2011 Fundamental chemistry and engineering aspects of post-treatment processes for desalinated water - A review. *Desalination* **273** (1), 6–22.

Bonds, R. W. 2005 Cement-mortar linings for ductile iron pipe. Available at: www.dipra.org/pdf/cementMortarLinings.pdf (accessed 1 November 2012).

Catling, L. A., Abubakar, I., Lake, I. R., Swift, L. & Hunter, P. R. 2008 A systematic review of analytical observational studies investigating the association between cardiovascular disease and drinking water hardness. *J. Water Health* **6** (4), 433–442.

Chang, P. H. 2004 The optimal control for corrosive effluent from the seawater desalination plant. Master thesis, National Cheng Kung University, Tainan City, Taiwan.

Chiu, H. F., Tsai, Sh., Chen, P. Sh., Wu, Tr. N. & Yang, Ch. Y. 2011 Does calcium in drinking water modify the association between nitrate in drinking water and risk of death from colon cancer? *J. Water Health* **9** (3), 498–506.

Cotruvo, J. 2006 Health aspects of calcium and magnesium in drinking water. In: *Proc. Int. Symp. on Health Aspects of Calcium and Magnesium in Drink*. Water, Baltimore, MD, USA, April 24–26.

Douglas, S. S. 2007 *Post Treatment Alternatives for Stabilizing Desalinated Water*. University of Central Florida, Orlando, FL.

Gerke, T. L., Maynard, B. J., Shock, M. R. & Lytle, D. L. 2008 Physiochemical characterization of five iron tubercles from a single drinking water distribution system: Possible new insights on their formation and growth. *Corrosion Sci*. **50** (7), 2030–2039.

Hasson, D. & Bendrihem, O. 2006 Modeling remineralization of desalinated water by limestone dissolution. *Desalination* **190** (1–3), 189–200.

Kozisek, F. 2003 Health Significance of Drinking Water Calcium and Magnesium. Available at: www.alkaway.com.au/downloads/hard-water-report.pdf. (accessed 24 January 2013).

Lahav, O. & Birnhack, L. 2008 Quality criteria for desalinated water and introduction of a novel, cost effective and advantageous post treatment process. *Desalination* **221** (1–3), 70–83.

Lee, J. E. & Schwab, K. J. 2005 Deficiencies in drinking water distribution systems in developing countries. *J. Water Health* **3** (2), 109–127.

Liang, J., Deng, A. Q., Xie, R. J., Gomez, M., Hu, J. Y., Zhang, J. F., Ong, Ch. N. & Adin, A. 2013 Impact of seawater reverse osmosis (SWRO) product remineralization on the corrosion rate of water distribution pipeline materials. *Desalination* **311**, 54–61.

Liu, Z. H., Yuan, D. X. & Dreybrodt, W. 2005 Comparative study of dissolution rate-determining mechanisms of limestone and dolomite. *Environ. Geol*. **49** (2), 274–279.

Penn, R., Birnhack, L., Adin, A. & Lahav, O. 2009 New desalinated drinking water regulations are met by an innovative post-treatment process for improved public health. *WST: Water Supply* **9** (3), 225–231.

Reynaud, A. 2010 Corrosion of cast irons. In: *Shreir's Corrosion*. (T. Richardson, ed.) Elsevier, Oxford, pp. 1737–1788.

Sarin, P., Snoeyink, V. L., Lytle, D. A. & Kriven, W. M. 2004 Iron corrosion scales: model for scale growth, iron release, and colored water formation. *J. Environ. Eng*. **4**, 364–373.

Tang, Z., Hong, S., Xiao, W. & Taylor, J. 2006 Characteristics of iron corrosion scales established under blending of ground, surface, and saline waters and their impacts on iron release in the pipe distribution system. *Corrosion Sci*. **48**, 322–342.

World Health Organization 2009 *Calcium and Magnesium in Drinking Water: Public Health Significance*, 1st edn. World Health Organization, Geneva, Switzerland, p. 190.

First received 13 February 2013; accepted in revised form 20 August 2013. Available online 20 September 2013